

A Novel Study of Neutron Structure Function F_2^n from Maximum Entropy Method

Chengdong Han,^{1,2} Rong Wang,^{1,2,*} and Xurong Chen^{1,2,3,†}

¹*Institute of Modern Physics, Chinese Academy of Sciences, Lanzhou 730000, China*

²*School of Nuclear Science and Technology, University of Chinese Academy of Sciences, Beijing 100049, China*

³*Guangdong Provincial Key Laboratory of Nuclear Science, Institute of Quantum Matter, South China Normal University, Guangzhou 510006, China*

We apply the Maximum Entropy Method to determine valence quark distributions of the neutron at a low scale Q_0^2 . At the initial evolution scale Q_0^2 , there are no sea quark and gluon distributions except for that of the three valence quarks (udd). Using the DGLAP equations with parton-parton recombination corrections (nonlinear effect), we obtain the neutron structure function F_2^n at any high scale Q^2 . The predicted structure function ratio F_2^n/F_2^p is approximately consistent with the world DIS data of proton and deuteron targets, if the uncertainties caused by model-dependent corrections are taken into account. Furthermore, our obtained F_2^n/F_2^p ratio basically agrees with BONuS experimental results after considering both the contamination from the nucleon resonances around $x \gtrsim 0.4, 0.5, 0.6$ and the contribution of systematic uncertainties. The predicted F_2^n/F_2^p and u/d ratios under the limit of $x \rightarrow 1$ are compared with the theoretical calculations. Finally, we check that the parton distributions of proton and neutron approximately satisfy isospin symmetry in this work.

PACS numbers: 12.38.-t, 13.15.+g, 13.60.Hb, 14.20Dh

I. INTRODUCTION

Determination of neutron structure function F_2^n [1–10] is vital for understanding the quark structure of the nucleon. In addition, much less known neutron structure information than proton due to the lack of neutron target makes the study of F_2^n a hot topic. At present, most of the structure function information of neutron is obtained through reviewed the world deep-inelastic scattering (DIS) data from the proton and deuteron (or ^3He) targets over the full available kinematics and considering some different nuclear correction models. Recently, the Barely Off-shell Nucleon Structure (BONuS) at Jefferson Lab experiment [5, 7, 11] measured the quasi-free neutron structure function data in both the nucleon-resonance and DIS regions by detecting low-momentum spectator protons at backward angles from the semi-inclusive scattering of electron with deuteron. Furthermore, over the past few decades, researchers have been interested in the ratio of structure functions F_2^n/F_2^p at very large Bjorken scaling variable x . The neutron structure function F_2^n or the F_2^n/F_2^p ratio is considered to be one of the best ways to determine the d/u (u/d for neutron) ratio at the $x \rightarrow 1$ limit.

These data analysis results of neutron structure functions described above do not come from the authentic free neutron. Since the absence of free neutron target because of the short lifetime of neutron and neutron beams are too low in energy or intensity, that makes it impossible to directly study its internal structure experimentally. Due to deuteron and helium (^3He) are relatively weakly bound, neutron structure information is usually extracted from data on deuterium or ^3He target via DIS measurement. The neutron structure function is then obtained by subtracting the known proton structure function from the deuteron or ^3He structure function after requir-

ing some model-dependent corrections, such as nuclear binding, Fermi motion, EMC effects, final state interactions or nucleon off-shell effects [12–16]. Of course, the extraction of the neutron structure function F_2^n after considering these nuclear medium effect corrections still have some uncertainties, especially in the large x region ($x > 0.8$). Different nuclear correction models give various theoretical predictions of the F_2^n/F_2^p and d/u (u/d for neutron) ratio at $x \rightarrow 1$ limit [3, 6, 17, 18].

In this work, we try to determine the initial valence quark distributions at Q_0^2 of neutron with Maximum Entropy Method (MEM), which is based on some already known structure information and properties of the neutron in the QCD theory and Quark Model. The MEM has been successfully applied to the studies of the parton distributions of proton [19, 20] and meson [21]. Taking the DGLAP equations with nonlinear corrections [22–25] to evolve the nonperturbative input of neutron obtained by MEM to a high scale, the obtained neutron structure function and F_2^n/F_2^p ratio are compared with some experimental data in this work. Then we render some discussions of our obtained structure function ratio F_2^n/F_2^p , u/d ratio of neutron with the results of different theoretical models at the limit of $x \rightarrow 1$. At last, we calculate the valence quark momentum distribution difference between proton and neutron with respect to Bjorken scaling variable x and the first moment difference between proton and neutron as a function of Q^2 to check that the proton and the neutron satisfy the isospin symmetry.

II. DETERMINE THE SIMPLE NONPERTURBATIVE INPUT BY MAXIMUM ENTROPY METHOD

The definition for Quark Model is a classification scheme that expounds the quantum numbers of the baryons and mesons by assuming that baryons are composed of three valence quarks and mesons are composed of a pair of quark and anti-quark. The parton distribution functions (PDFs) of nucleon at high Q^2 obtained by performing DGLAP equations

*Electronic address: rwang@impcas.ac.cn

†Electronic address: xchen@impcas.ac.cn

with parton-parton recombinations depend on the initial parton distributions at low scale Q_0^2 . In this analysis, a naive non-perturbative input of the neutron only contains three valence quarks without other nonperturbative components (sea quarks and gluons), which is the simplest initial parton distribution input [22, 26–28]. In the view of dynamical PDF model, the sea quarks and gluons are radiatively generated from three valence quarks of neutron at high scale $Q^2 > Q_0^2$. We take the input scale $Q_0^2 = 0.067 \text{ GeV}^2$ that is determined by the global QCD analysis of experimental data of proton [24]. The running strong coupling and parton-parton correlation length R which characterizes the strength parton-parton recombination corrections are determined by a large number of DIS experimental data at high Q^2 [24, 29], which are the same as in the paper of valence quark distributions of the proton from MEM by Wang and Chen [19].

The most general function form to approximate valence quark distribution of neutron is the time-honored canonical parametrization $f(x) = Ax^B(1-x)^C$ [30]. Therefore, the parametrization of nonperturbative input in this analysis is as follows:

$$\begin{aligned} u_v(x, Q_0^2) &= A_u x^{B_u} (1-x)^{C_u}, \\ d_v(x, Q_0^2) &= A_d x^{B_d} (1-x)^{C_d}. \end{aligned} \quad (1)$$

According to the framework of Quark Model, we have the valence sum rules and the momentum sum rule as constraints:

$$\int_0^1 u_v(x, Q_0^2) dx = 1, \quad \int_0^1 d_v(x, Q_0^2) dx = 2. \quad (2)$$

$$\int_0^1 x[u_v(x, Q_0^2) + d_v(x, Q_0^2)] dx = 1. \quad (3)$$

The quark confinement is a typical feature of strong interaction in Non-Abelian gauge field theory [31], which means all quarks are confined in a small region of hadron size. In this work, we use the Heisenberg uncertainty principle Eq. (4) as the constraint [19],

$$\sigma_X \sigma_P \geq \frac{\hbar}{2}, \quad (4)$$

where the σ_X is the standard deviation of the spacial distribution of one valence quark in the neutron, and the σ_P is the standard deviation of the valence quark momentum distribution in the neutron. Here, σ_X is directly related to the magnetic radius (R_m) of the neutron, which is 0.864 fm [32]. A simple estimation of σ_X is $\sigma_X = (2\pi R_m^3/3)/(\pi R_m^2) = 2R_m/3$, for the sphere neutron. In addition, σ_X of each d valence quark is divided by $2^{1/3}$ as there are two d valence quarks in the neutron. Then we get $\sigma_{X_u} = 2R_m/3$ and $\sigma_{X_d} = 2R_m/(3 \times 2^{1/3})$ for u and d valence quarks inside neutron respectively [19, 33]. Furthermore, the standard deviation of momentum fraction x at initial scale Q_0^2 is defined as follows,

$$\sigma_x = \frac{\sigma_P}{M_n}, \quad (5)$$

where M_n is the rest mass of neutron [32]. Finally, the constraints for valence quark distributions from QCD color confinement and Heisenberg uncertainty principle [19] are written as,

$$\begin{aligned} \sqrt{\langle x_u^2 \rangle - \langle x_u \rangle^2} &= \sigma_{x_u}, & \sqrt{\langle x_d^2 \rangle - \langle x_d \rangle^2} &= \sigma_{x_d} \\ \langle x_u \rangle &= \int_0^1 x u_v(x, Q_0^2) dx, & \langle x_d \rangle &= \int_0^1 x \frac{d_v(x, Q_0^2)}{2} dx \\ \langle x_u^2 \rangle &= \int_0^1 x^2 u_v(x, Q_0^2) dx, & \langle x_d^2 \rangle &= \int_0^1 x^2 \frac{d_v(x, Q_0^2)}{2} dx. \end{aligned} \quad (6)$$

According to the constraints (Eqs. (2), (3), (4), (5) and (6)) already introduced above, there is only one unknown parameter B_u for Eq.(1). By applying MEM, one can determine the reasonable valence quark distributions under these constraints. The generalized information entropy of valence quark distributions for neutron is given by,

$$\begin{aligned} S &= - \int_0^1 \left[u_v(x, Q_0^2) \text{Ln}(u_v(x, Q_0^2)) \right. \\ &\quad \left. + 2 \frac{d_v(x, Q_0^2)}{2} \text{Ln} \left(\frac{d_v(x, Q_0^2)}{2} \right) \right] dx. \end{aligned} \quad (7)$$

The optimal parameterized initial valence quark distributions are given when the entropy S value is at the maximum. Fig. 1 shows the information entropy S of the valence quarks at the input scale Q_0^2 as a function of the free parameter B_u . Entropy S value peaks at $B_u = 0.482$. Hence the corresponding valence quark distributions from MEM are given by,

$$\begin{aligned} u_v(x, Q_0^2) &= 8.188 x^{0.482} (1-x)^{2.581}, \\ d_v(x, Q_0^2) &= 5.082 x^{0.138} (1-x)^{1.080}. \end{aligned} \quad (8)$$

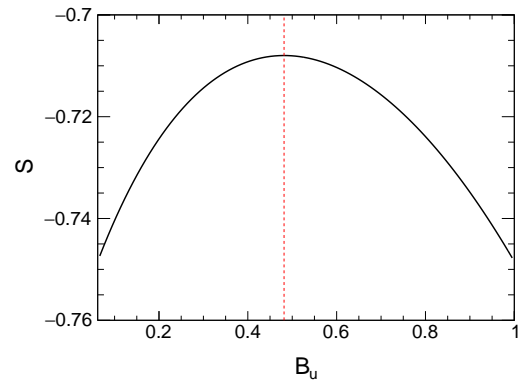


FIG. 1: Entropy S of valence quark distributions of neutron at $Q_0^2 = 0.064 \text{ GeV}^2$ is plotted as a function of the free parameter B_u .

III. RESULTS AND DISCUSSIONS

Parton distribution functions of neutron are evaluated dynamically starting from the obtained three valence quark input at the low scale Q_0^2 . By performing DGLAP equations

[34–36] with parton-parton recombination corrections [22–25], the parton distributions at an arbitrarily high scale Q^2 can be determined with the nonperturbative input (Eq. (8)). Fig. 2 shows the predicted momentum distributions of up and down valence quarks, sea quarks and gluon, at $Q^2 = 12 \text{ GeV}^2$.

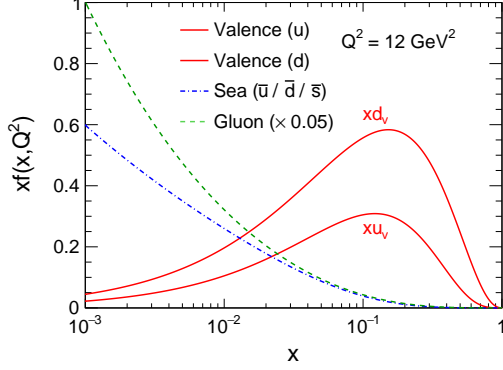


FIG. 2: The predicted valence quark, sea quark and gluon distributions at $Q^2 = 12 \text{ GeV}^2$ by performing DGLAP evolution equations with the parton-parton recombination corrections to the pure valence quark nonperturbative input from MEM.

The structure functions of nucleon reflect the characteristics of QCD defined by the asymptotic freedom of short distances and the confinement of quarks on the long distance scale. The unpolarized structure function $F_2(x)$ is directly related to the quark distribution functions. According to the Quark-Parton model, the structure function [37] is written as,

$$2xF_1(x) = F_2(x) = \sum_i e_i^2 x f_i(x), \quad (9)$$

where the subscript i is flavor index, e_i is the electrical charge of the quark flavor i , and $x f_i(x)$ is the momentum fraction distribution of the quark of flavor i . Since valence quarks dominate in the large x region ($x > 0.1$), the $F_2(x)$ at large x mainly comes from the contribution of valence quarks. In the small x region ($x < 0.1$), the sea quarks begin to make an important contribution to the structure function $F_2(x)$.

The BONuS experiment at Jefferson Lab [5, 7] is via tagging very low momentum spectator protons to measure the F_2^n of the nearly free neutron from the semi-inclusive scattering of electron off the deuterium. This experimental method minimizes the off-shell effect significantly and reduces the nuclear binding uncertainties by picking the spectator protons of momentum below 100 MeV/c and backward angles greater than 100° . These selections ensure that the scattering occurs on the nearly free neutrons. The current F_2^n data collection cover the nucleon-resonance and deep-inelastic regions with a wide range of Bjorken scaling variable x under $0.65 < Q^2 < 4.52 \text{ GeV}^2$. Fig. 3 presents our determined F_2^n as a function of x compared with BONuS measurements, where the dashed curve only includes the contribution of valence quarks and the solid curve includes the sum of valence quarks and sea quarks. And the Analysis 1 of BONuS experiment is from the Monte

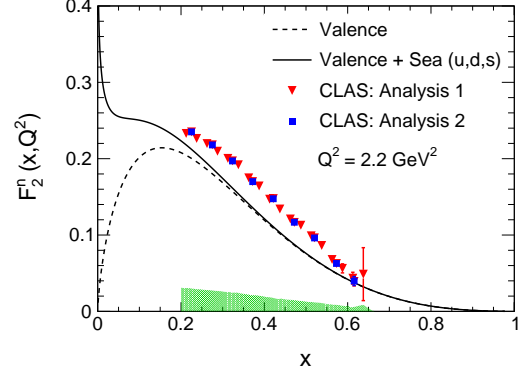


FIG. 3: The predicted structure function of neutron F_2^n as a function of Bjorken x compared with the BONuS experiment, where Analysis 1 (triangles) of BONuS experiment performs the Monte Carlo method and the Analysis 2 (squares) performs the ratio method. The solid curve includes the contribution of the sea quarks and the valence quarks, while the dashed curve includes only the valence quark contribution. The systematic uncertainties of the Monte Carlo method in F_2^n extraction are shown as the green shaded band [7].

Carlo method and the Analysis 2 is from the ratio method. By comparisons, our MEM predictions are consistent with the BONuS data within the systematic uncertainties.

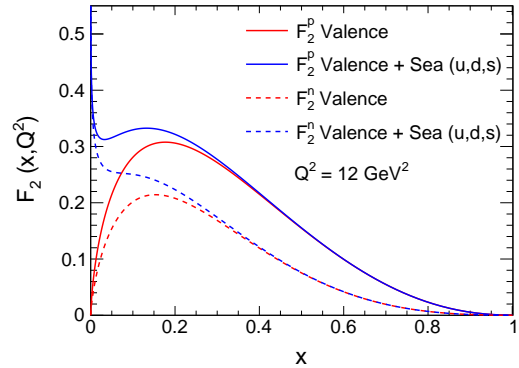


FIG. 4: Comparisons of the structure functions of proton (solid curve) and neutron (dashed curve). The structure function calculations are performed with and without the sea quark distribution.

Fig. 4 shows the comparisons between the predicted proton structure function and the predicted neutron structure function, from MEM. The predictions for the proton is taken from a previous work [19]. We see that the sea quark distributions only contribute significantly in the small x region.

Fig. 5 shows the predicted ratio F_2^n/F_2^p by MEM as a function x , compared with the previous measurements of the scatterings on deuteron and proton. NMC data is the DIS measurement by the muon beam scattering on the hydrogen and deuterium [1]. The data by J. Arrington et al. is a new and systematical analysis of the neutron structure function from

the deuteron and proton data considering the impulse assumption and an effective two-nucleon mass operator [2]. The full squares show the F_2^n/F_2^p data extracted by applying the deuteron in-medium correction [3]. In Fig. 5, our predicted structure function ratio F_2^n/F_2^p is a little bit lower than the data, but still consistent with the experimental data. In order to extract the free neutron information from the deuteron, some models of nuclear corrections should be considered, such as the nuclear density dependent EMC effect [13, 14], Fermi motion [13], on-shell model extractions [15] and off-shell correction [12, 16]. The problem of these corrections is that the deuteron or ^3He , even if only weakly bound, are not the real free neutron-proton systems. Furthermore, using different nuclear correction models can lead to some significant uncertainties for the ratio F_2^n/F_2^p at the $x \rightarrow 1$ limit.

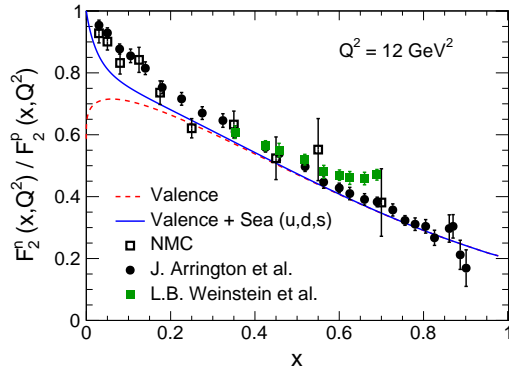


FIG. 5: The obtained structure function ratio of neutron to proton F_2^n/F_2^p from MEM, compared with the previous experimental extractions. NMC data (open squares) are extracted from the simultaneous measurements on hydrogen and deuterium with the incident muon beam [1]. The analysis by J. Arrington et al. (circles) are corrected with the nucleon motion in deuterium [2]. The full squares show F_2^n/F_2^p data extracted from the deuteron in-medium correction [3]. The errors plotted display the total experimental uncertainties.

Fig. 6 shows the predicted ratio F_2^n/F_2^p at $Q^2 = 2.2 \text{ GeV}^2$ compared with the BONuS experiment of three different cuts on W^* . W^* here denotes the invariant mass of the final hadrons. The cyan band of the prediction shows the variation of the Q^2 -dependence from 1 GeV^2 to 4.3 GeV^2 . In Fig. 6, there is a discrepancy between our prediction and the BONuS data. Nevertheless our calculation agree with the data of large W^* around $x \sim 0.2$ and $x \sim 0.6$. We argue that: (1). The nonperturbative quark-gluon interactions are significant and the inclusive lepton-nucleon cross section is dominated by nucleon-resonance at lower energy [8]. We can see the obvious hadron resonance peaks in BONuS data in the $0.4 < x < 0.7$ region, even under the cut of $W^* > 1.8 \text{ GeV}$. The future BONuS12 data with the electron energy upgrade are expected to remove the discrepancy. (2). The discrepancy will be removed if the relatively big systematic errors of BONuS are taken into account. In short, the MEM prediction of the ratio F_2^n/F_2^p is close to the BONuS measurement

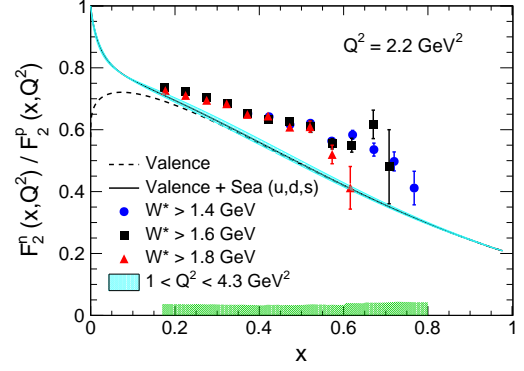


FIG. 6: Comparisons of our predicted F_2^n/F_2^p ratio with the BONuS experiment of three different W^* cuts. The error bars show only the statistical uncertainties of the data. The total systematic uncertainties of BONuS experiment are demonstrated at the bottom (green band) [7]. Our theoretical prediction is at $Q^2 = 2.2 \text{ GeV}^2$, and the cyan band shows the variation of the scale evolution from 1 GeV^2 to 4.3 GeV^2 (in accordance with the experimental data).

if the quark-hadron duality correction [8] and the systematic uncertainties are considered.

The u/d ratio is a quantity which is directly related to the ratio F_2^n/F_2^p . Fig. 7 shows the predicted u/d ratio as a function of x at $Q^2 = 10 \text{ GeV}^2$. MEM in this work gives $u/d = 0$ at the limit of x approaching one. In experiment, the d/u ratio of the proton is usually extracted from the F_2^n/F_2^p data, neglecting the strange quark contribution. Note that the d/u ratio of the proton equals the u/d ratio of the neutron under the assumption of isospin symmetry.

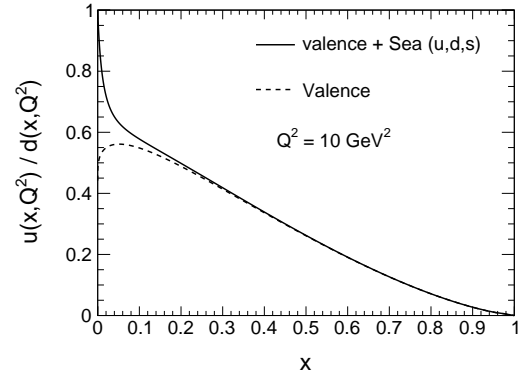


FIG. 7: The u/d ratio of the neutron at $Q^2 = 10 \text{ GeV}^2$ given by MEM. The solid curve includes also the sea quark contributions, while the dashed curve is calculated from the valence quark distributions only.

Table I lists the comparisons of our predicted F_2^n/F_2^p ratio and u/d ratio of neutron at the limit of $x \rightarrow 1$, compared with other theoretical predictions. The structure function ratio between neutron and proton is denoted as $R^{n/p}(x) = F_2^n(x)/F_2^p(x)$

TABLE I: The list of the theoretical predictions of $R^{n/p} = F_2^n/F_2^p$ and u^n/d^n at the limit of $x \rightarrow 1$ from different models.

	$R^{n/p}$	u^n/d^n
SU(6) Flavor Symmetry	2/3	1/2
Perturbative QCD	3/7	1/5
Quark Counting Rule	3/7	1/5
Diquark / Feynman	1/4	0
Quark Model / Isgur	1/4	0
MEM (this work)	0.2	0

in this work for the convenience of discussions. In this work by MEM, we find that $R^{n/p}(0) \approx 1$ to $R^{n/p}(1) \approx 0.2$, which is clearly depicted in Fig. 5. $R^{n/p}(0) \approx 1$ is due to the fact that the sea quark distribution dominates at small x . The other result is that $u^n/d^n \approx 0$ when x approaches one. Our result is quite different from the predictions from the exact spin-flavor SU(6) symmetry, the perturbative QCD assuming the helicity conserved quarks interacted via hard gluon exchange [38], and the quark counting rule method. However the models with the SU(6) symmetry breaking via the scalar diquark dominance [39, 40] predict the very similar result of ours. These predictions at large x are needed to be tested in the future experiments.

To check the isospin symmetry between proton and neutron, the difference of the valence quark distributions and the moments of the distributions are presented in Fig. 8. The barely difference between xu_v^p and xd_v^n is from the difference between the proton radius and the neutron radius used in the maximum entropy method. The conclusion is that the isospin symmetry between proton and neutron is a very good symmetry in terms of parton distributions.

IV. SUMMARY

The maximum entropy method offers a simple and novel way to estimate the nonperturbative structure of nucleon. The predictions of the valence structures of both proton and neutron are consistent with the current experimental data. The measurement of the nearly free neutron by BONuS collaboration is an important test of our prediction. The future measurement at a higher beam energy is highly needed [41], for the high energy measurement will remove the contamination of the nucleon resonances, so as to clearly test the prediction on the ratio F_2^n/F_2^p . Moreover, the different predictions on the up and down valence quark distributions from different

models will be differentiated by the MARATHON measurement at JLab [42]. Last but not least, the widely discussed electron-ion colliders [43–45] will play an important role in understanding the structure of neutron.

Based on the estimations of MEM in this work, we see that the neutron structure and the proton structure well satisfy the isospin symmetry. The large- x behaviors of F_2^n/F_2^p and u^n/d^n predicted by MEM are close to the diquark model and the

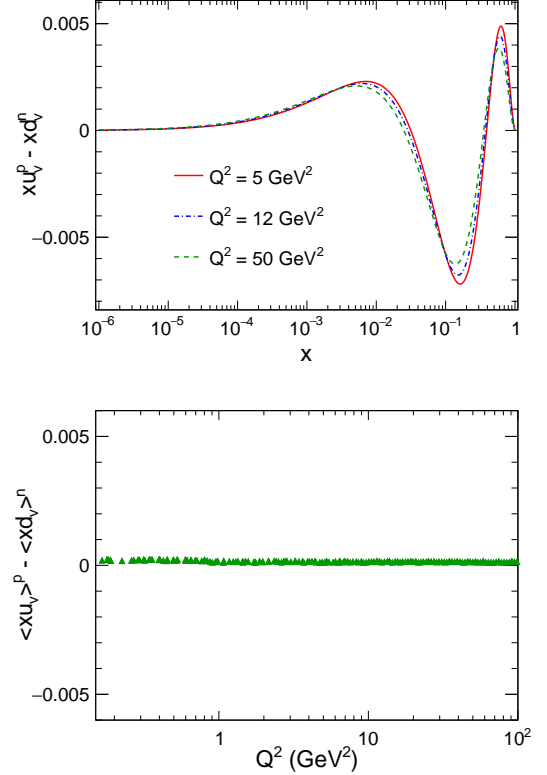


FIG. 8: (Up panel) The valence quark difference between proton and neutron as a function of Bjorken variable x . (Down panel) The difference of the moments of valence quark distributions between proton and neutron as a function of Q^2 .

simple quark model predictions, but deviated from the perturbative QCD prediction. There is still room for some improvements of MEM, such as including more constraints from the QCD dynamics.

Acknowledgments: This work is supported by the Strategic Priority Research Program of Chinese Academy of Sciences under Grant No. XDB34030301.

-
- [1] P. Amaudruz et al., The New Muon Collaboration (NMC), Nucl. Phys. B 371 (1992) 3.
 - [2] J. Arrington, F. Coester, R. J. Holt, and T.-S. H. Lee, J. Phys. G: Nucl. Part. Phys. 36 (2009) 025005.
 - [3] L. B. Weinstein et al., Phys. Rev. Lett. 106 (2011) 052301.

- [4] J. Arrington, J. G. Rubin, and W. Melnitchouk, Phys. Rev. Lett. 108 (2012) 252001.
- [5] N. Baillie, et al., (The CLAS Collaboration), Phys. Rev. Lett. 108 (2012) 142001.
- [6] O. Hen, E. Piasetzky, R. Shneor, L. B. Weinstein, D. W. Higin-

- botham, arXiv: 1109.6197.
- [7] S. Tkachenko, et al., (The CLAS Collaboration), Phys. Rev. C 89 (2014) 045206.
 - [8] I. Niculescu et al., Phys. Rev. C 91 (2015) 055206.
 - [9] A. Accardi, L. T. Brady, W. Melnitchouk, J. F. Owens, and N. Sato, Phys. Rev. C 91 (2016) 114017.
 - [10] H. Szumila-Vance, C.E. Keppel, S. Escalante, N. Kalantarians, arXiv:2002.02597v3.
 - [11] H. Fenker et al., Nucl. Instrum. Methods Phys. Res. A 592 (2008) 273.
 - [12] W. Melnitchouk, and A. W. Thomas, Phys. Lett. B 377 (1996) 11.
 - [13] L. W. Whitlow, E. M. Riordan, S. Dasu, S. Rock, and A. Bodek, Phys. Lett. B 282 (1992) 475.
 - [14] L. L. Frankfurt, and M. I. Strikman, Phys. Rept. 160 (1988) 235.
 - [15] J. Gomez et al., Phys. Rev. D 49 (1994) 4348.
 - [16] W. Melnitchouk, A. W. Schreiber, and A. W. Thomas, Phys. Lett. B 335 (1994) 11.
 - [17] K. Nakano, and S. S. M. Wong, Nucl. Phys. A 530 (1991) 555.
 - [18] R. J. Holt and C. D. Roberts, Rev. Mod. Phys. 82 (2010) 2991.
 - [19] R. Wang, X. R. Chen, Phys. Rev. D 91 (2015) 054026.
 - [20] C. D. Han, X. R. Chen, Chin. Physics C, 41 (2017) 113103.
 - [21] C. D. Han, H. Y. Xing, X. P. Wang, Q. Fu, R. Wang, X. R. Chen, Phys. Lett. B 800 (2020) 135066.
 - [22] X. Chen, J. Ruan, R. Wang, W. Zhu, and P. Zhang, Int. J. Mod. Phys. E 23 (2014) 1450057.
 - [23] R. Wang, X. Chen and Q. Fu, Nucl. Phys. B 920 (2017) 1.
 - [24] R. Wang and X. R. Chen, Chin. Phys. 41 (2017) 053103.
 - [25] W. Zhu, R. Wang, J. H. Ruan, X. R. Chen, P. M. Zhang, Eur. Phys. J. Plus 131 (2016) 6.
 - [26] G. Parisi and R. Petronzio, Phys. Lett. B 62 (1976) 331.
 - [27] V. A. Novikov, M. A. Shifman, A. I. Vainshtein, and V. I. Zakharov, JETP Lett. 24 (1976) 341.
 - [28] M. Glück and E. Reya, Nucl. Phys. B 130 (1977) 76.
 - [29] M. Glück, E. Reya, and A. Vogt, Eur. Phys. J. C 5 (1998) 461.
 - [30] J. Pumplin, D. R. Stump, J. Huston, H. L. Lai, P. Nadolsky, and W. K. Tung, J. High Energy Phys. 07 (2002) 012.
 - [31] Kenneth G. Wilson, Phys. Rev. D 10 (1974) 2445.
 - [32] P.A. Zyla et al. (Particle Data Group), Prog. Theor. Exp. Phys. (2020) 083C01.
 - [33] C. D. Han and X. R. Chen, Chin. Phys. C 41 (2017) 113103.
 - [34] Y. L. Dokshitzer, Sov. Phys. JETP 46 (1977) 641.
 - [35] V. N. Gribov, L. N. Lipatov, Sov. J. Nucl. Phys. 15 (1972) 438.
 - [36] G. Altarelli, G. Parisi, Nucl. Phys. B 126 (1977) 298.
 - [37] C. G. Callan, D. J. Gross, Phys. Rev. Lett. 22 (1969) 156.
 - [38] G. R. Farrar and D. R. Jackson, Phys. Rev. Lett. 35 (1975) 1416.
 - [39] R. P. Feynman, Photon Hadron Interactions (Benjamin, Reading, MA, 1972).
 - [40] F. E. Close, Phys. Lett. B 43 (1973) 422.
 - [41] Carlos Ayerbe-Gayoso, on behalf of the CLAS Collaboration, 23rd International Spin Physics Symposium - SPIN2018, (2018).
 - [42] J. Arrington et al., Jefferson Lab PAC37 Proposal (https://www.jlab.org/exp_prog/proposals/10/PR12-10-103.pdf), (2010).
 - [43] A. Accardi et al., Eur. Phys. J. A 52 (2016) 268.
 - [44] X. R. Chen, arXiv: 1809.00448.
 - [45] Xurong Chen, Feng-Kun Guo, Craig D. Roberts, Rong Wang, arXiv:2008.00102.